

Supplementary Figures:

$\alpha 2\delta$ expression sets presynaptic calcium channel abundance and release probability. Hoppa et al.

Figure S1. Validation of anti- $\alpha 1_A$ immunostaining by shRNA-mediated knockdown of $\alpha 1_A$. **a**, Confocal immunofluorescence images of a representative neuronal cell soma without (top) or with (bottom) transfection of vGpH+shRNA $\alpha 1_A$ and stained for anti-GFP (green; left) and anti- $\alpha 1_A$ (pseudo-colored; right) taken from the same dish. On average the background-corrected fluorescence intensity was reduced to $28 \pm 11\%$ in shRNA-transfected neurons compared to adjacent non-transfected controls (n=6). Scale bar = 10 μm . **b**, Confocal immunofluorescence images of a representative set of presynaptic boutons transfected with vGpH+shRNA $\alpha 1_A$ and stained for anti-GFP (green; left) and anti- $\alpha 1_A$ (pseudo-colored; right). Bouton regions are indicated by the white circles and show little obvious fluorescence accumulation of anti- $\alpha 1_A$ staining in shRNA-transfected cells compared to either non-transfected immune-positive puncta or control transfections (Fig. 1d). Scale bar = 2 μm .

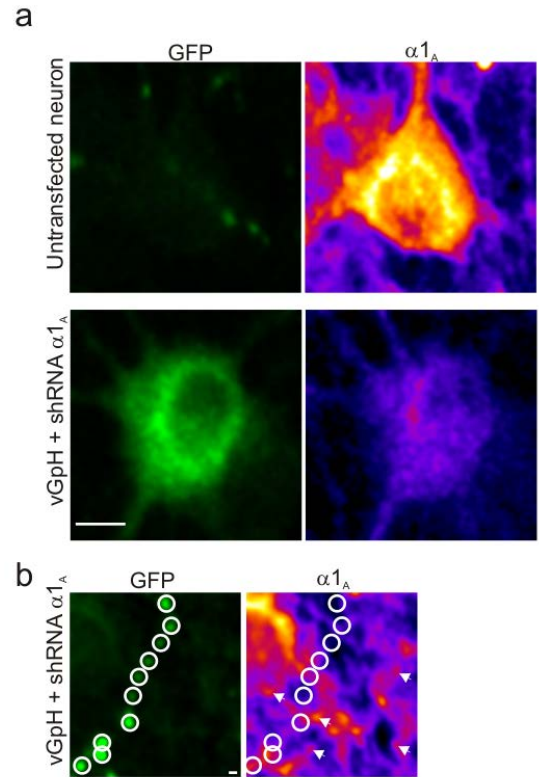


Figure S2. Expression of eGFP- $\alpha 1_A$ leads to two-fold increase in somatic $\alpha 1_A$. **a**, Confocal immunofluorescence images of a neuron transfected with eGFP- $\alpha 1_A$ and stained for anti-GFP (green; left) and anti- $\alpha 1_A$ (native+exogenous channels - pseudo-colored; right). **b**, Measurement of anti- $\alpha 1_A$ immunofluorescence intensity shows that transfection of eGFP- $\alpha 1_A$ leads to a significant increase ($F = 1369 \pm 172$ au, n=9) in the total amount of P/Q-type calcium channels in cell bodies compared to non-transfected cells ($F = 679 \pm 186$, n=16). Scale bar = 10 μm , pseudocoloured scale represents value of 0-2000 au. Values are mean \pm SEM, statistics determined by Student's t-test.

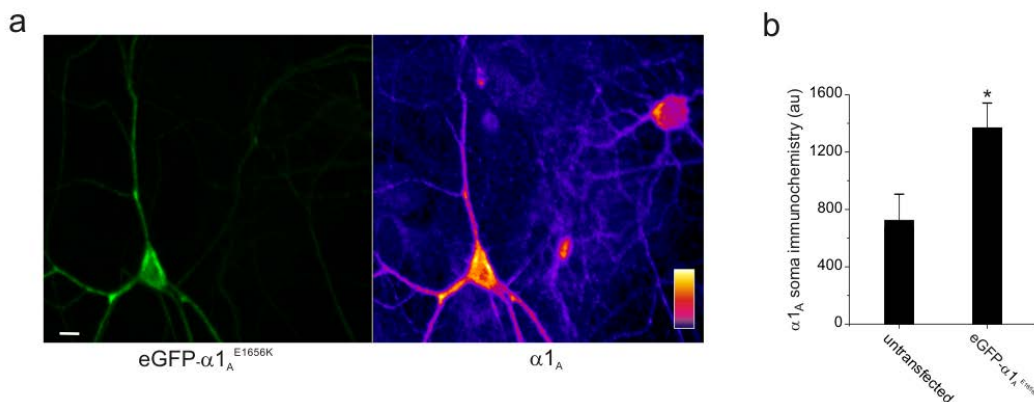


Figure S3. shRNA-mediated ablation of $\alpha 2\delta-1$ leads to depletion of synaptic $\alpha 1_A$.

We made use of co-transfection of VAMPmCh with or without shRNA-depletion of $\alpha 2\delta-1$ to examine more clearly the extent of synaptic $\alpha 1_A$ depletion caused by loss of $\alpha 2\delta-1$. Confocal immunofluorescence images using anti-GFP (top) and anti- $\alpha 1_A$ (bottom) antibodies. VAMPmCh-positive boutons generally show significant immunopositive $\alpha 1_A$ fluorescence in controls (left); however following shRNA-mediated $\alpha 2\delta-1$ depletion (right) no obvious immunostaining is apparent.

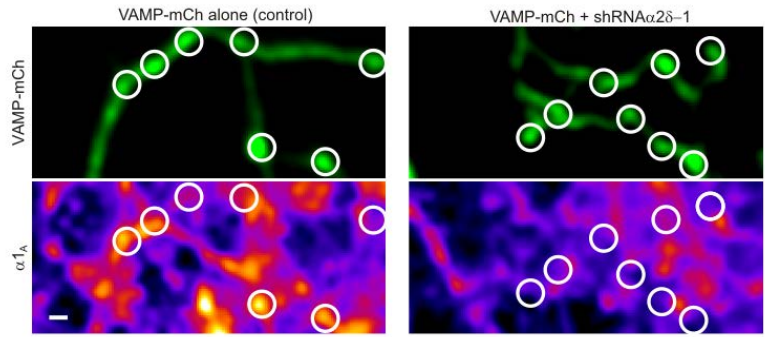
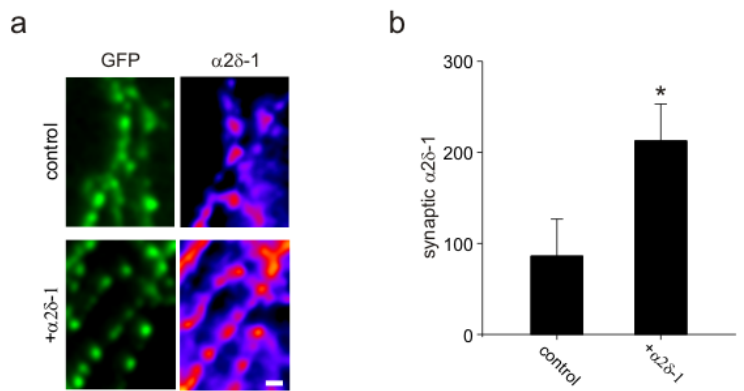


Figure S4: Overexpression of $\alpha 2\delta-1$ leads to a synaptic increase in $\alpha 2\delta-1$.

a, Confocal immunofluorescence images of a representative set of presynaptic boutons transfected with GCaMP alone (top) or GCaMP3 + $\alpha 2\delta-1$ (bottom) and stained for anti-GFP (green; left) and anti- $\alpha 2\delta-1$ (pseudo-colored; right). GCaMP3 was used to validate bouton function prior to fixation (see figure S5 for details of GCaMP3) scale bar **b**, Measurements of synaptic $\alpha 2\delta-1$ for GCaMP3 expressing synapses (86 ± 41) and GCaMP3 + $\alpha 2\delta-1$ (212 ± 40), $p < 0.05$ $n = 6$ and 7 respectively. Values are mean \pm SEM, statistics determined by Student's t-test



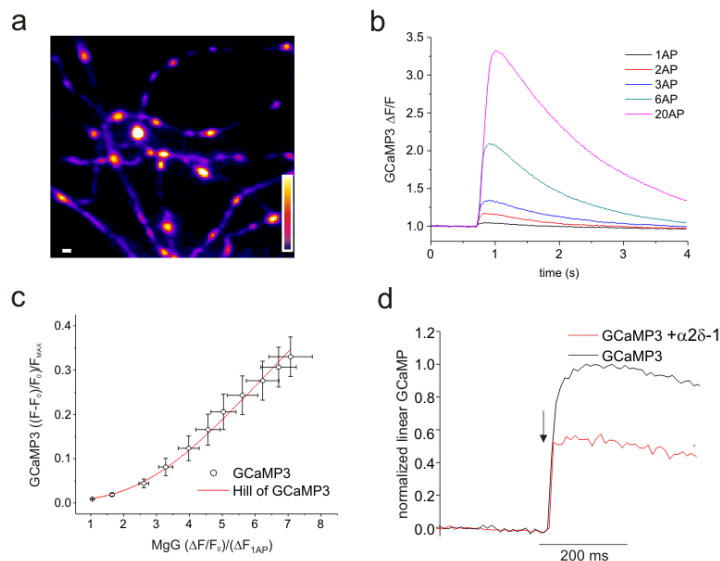
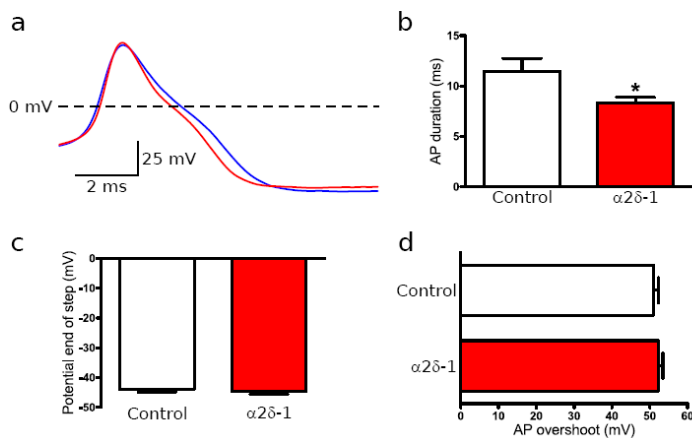


Figure S6. GCaMP3-based measurements shows expression of $\alpha 2\delta - 1$ reduces AP-driven Ca^{2+} influx at nerve terminals by ~2-fold. **a**, ΔF image obtained for a 10 AP (100 Hz) stimulus from a GCaMP3-transfected neuron's axonal field. **b**, example GCaMP3 traces recorded from 24 boutons in a single neuron with varying number of APs delivered at 100 Hz. **c**, GCaMP3 is a non-linear Ca^{2+} indicator. Comparison of the peak fluorescence for 1-7 AP stimulation obtained in GCaMP3-transfected or non-transfected MgG-loaded boutons ($n=11$ dishes) stimulated at 100 Hz² (all experiments were performed at 2 mM external Ca^{2+}). The

GCaMP3 signals are reported as the $\Delta F/F_{\max}$ where F_{\max} is measured from the saturating value obtained following treatment with ionomycin. The MgG data are normalized to the peak fluorescence obtained in the first AP. The relationship between GCaMP3 and MgG data were fit with a generalized Hill equation $y=x^n/(k^n+x^n)$. The fit yielded a Hill coefficient $n=2.46$ (adjusted $R^2=0.997$), in excellent agreement with that reported for GCaMP3 *in vitro*³. **d**, Single AP GCaMP3 responses from neurons co-transfected with (red) or without (black) $\alpha 2\delta - 1$. Responses were linearized (see Methods) to account for the non-linearity and normalized to the control response. The average peak values of normalized traces are GCaMP3 (1.0 ± 0.2 , $n=8$) alone and GCaMP3 + $\alpha 2\delta - 1$ (0.49 ± 0.18 , $n=8$) shows that co-expression of $\alpha 2\delta 1$ leads to a significant decrease ($p < 0.05$) in Ca^{2+} influx, in excellent agreement with data obtained using Fluo5F-AM loading (Fig. 3). Values are mean \pm SEM, statistics determined by Student's t-test.

Figure S6: Action Potential Measurements:

a, Example traces of action potential response to current pulse stimulation in DRG neurons. The action potential was terminated faster in DRG neurons transfected with $\alpha 2\delta - 1$ cDNA (red trace), compared to control cells transfected with empty vector (blue trace); YFP cDNA was used as a marker of transfection. **b**, Action potential duration. Transfection with $\alpha 2\delta - 1$ cDNA significantly shortened the action potential duration



measured from the peak of the action potential to the peak of the after-hyperpolarization (* $P < 0.05$, Student's t test, $N=45$ in both groups). A significant difference was also observed at 50 % action potential height ($P < 0.05$, data not shown). **c**, Action potential overshoot. The average action potential peak height was not altered by transfection with $\alpha 2\delta - 1$ cDNA, compared to control. **d**, the membrane potential measured at the end of the 400 ms trace was not affected by $\alpha 2\delta - 1$ (Control: -58.1 ± 0.8 mV; + $\alpha 2\delta - 1$: -58.9 ± 0.7 mV SEM)".

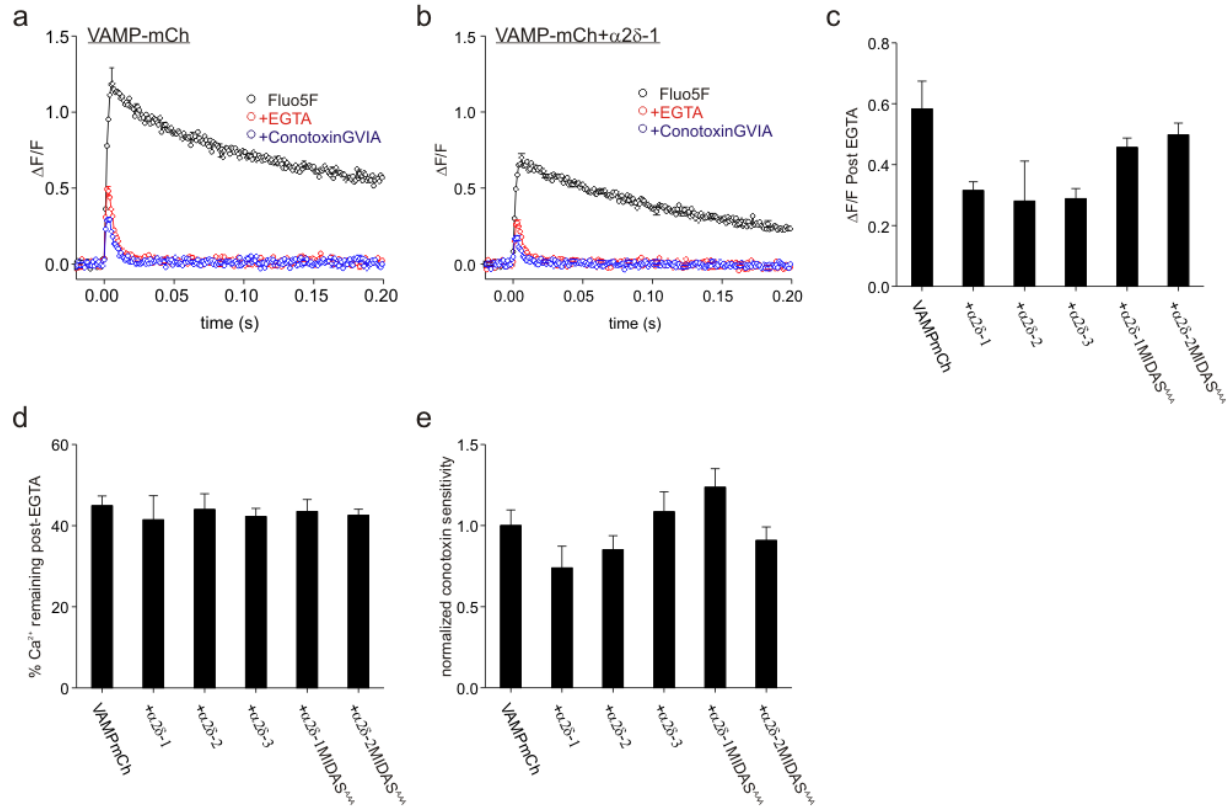


Figure S7. Voltage-gated Ca^{2+} channels subtypes are unaltered by $\alpha 2\delta$ expression. **a**, Average Ca^{2+} influx ($\Delta F/F$) in response to 1 AP from a cell transfected with VAMP-mCh (black), after loading with EGTA, (red), and after exposure to conotoxin GVIA (blue). **b**, The same as in (a) except that cells is transfected with VAMP-mCh + $\alpha 2\delta-1$. **c**, $\Delta F/F$ of Ca^{2+} transient after loading with EGTA: VAMP-mCh= 0.58 ± 0.09 ; VAMP-mCh+ $\alpha 2\delta-1=0.32 \pm 0.03$; VAMP-mCh+ $\alpha 2\delta-2=0.28 \pm 0.13$; VAMP-mCh+ $\alpha 2\delta-3=0.29 \pm 0.03$; VAMP-mCh+ $\alpha 2\delta-1$ MIDAS^{AAA}= 0.43 ± 0.03 ; VAMP-mCh+ $\alpha 2\delta-2$ MIDAS^{AAA}= 0.43 ± 0.01 . **d**, Percent of Ca^{2+} signal remaining after loading neurons with EGTA in response to a single action potential: VAMP-mCh= 45 ± 2.5 ; VAMP-mCh+ $\alpha 2\delta-1=41 \pm 5.9$; VAMP-mCh+ $\alpha 2\delta-2=44 \pm 3.9$; VAMP-mCh+ $\alpha 2\delta-3=42 \pm 2.0$; VAMP-mCh+ $\alpha 2\delta-1$ MIDAS^{AAA}= 43 ± 2.9 , VAMP-mCh+ $\alpha 2\delta-2$ MIDAS^{AAA}= 43 ± 1.5 . **e**, Fraction of Ca^{2+} influx sensitive to blockage with ω -conotoxin GVIA normalized to control (VAMP-mCh) cells. VAMP-mCh= 1 ± 0.1 ; VAMP-mCh+ $\alpha 2\delta-1=0.74 \pm 0.13$; VAMP-mCh+ $\alpha 2\delta-2=0.85 \pm 0.09$; VAMP-mCh+ $\alpha 2\delta-3=1.09 \pm 0.12$; VAMP-mCh+ $\alpha 2\delta-1$ MIDAS^{AAA}= 1.23 ± 0.11 ; VAMP-mCh+ $\alpha 2\delta-2$ MIDAS^{AAA}= 0.91 ± 0.08 . Values are mean \pm SEM ne5 for all measurements, (* $p < 0.05$) statistical significance was determined by one-way ANOVA with Tukey's HSD for Post-Hoc analysis.

Figure S8. $\alpha 2\delta$ -1 MIDAS motif is necessary to increase Ca^{2+} currents in a heterologous expression system.

a, Representative current traces resulting from step potentials from -90 mV to between -30 mV and +10 mV, in 5 mV increments for tsA-201 cells transfected with $\text{Ca}_v2.2/\beta 1b$ in the absence of $\alpha 2\delta$ (top panel) or the presence of wild-type $\alpha 2\delta$ -1, middle panel), or $\alpha 2\delta$ -1 MIDAS^{AAA} (bottom panel). **b**, IV relationships for cells transfected with $\text{Ca}_v2.2/\beta 1b$ in the absence of $\alpha 2\delta$ (□, n = 15) or the presence of wild-type $\alpha 2\delta$ -1 (●, n = 19), or $\alpha 2\delta$ -1 MIDAS^{AAA} (Δ, n = 16).

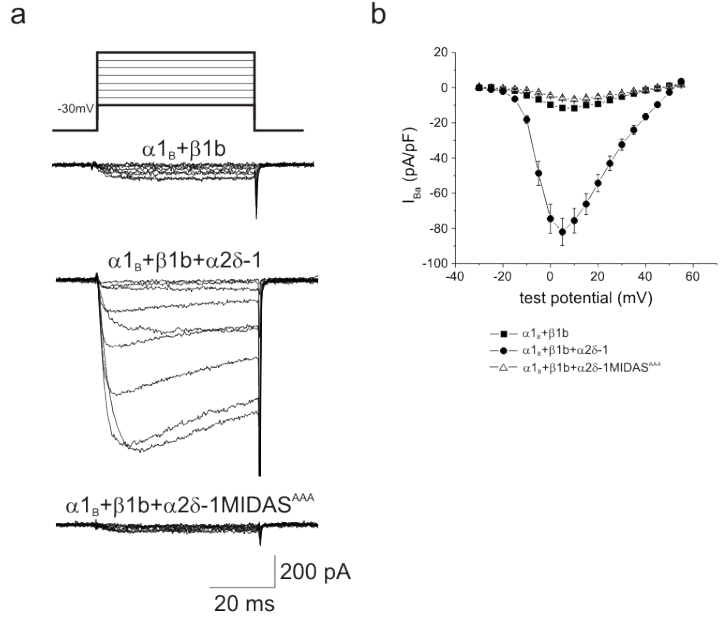
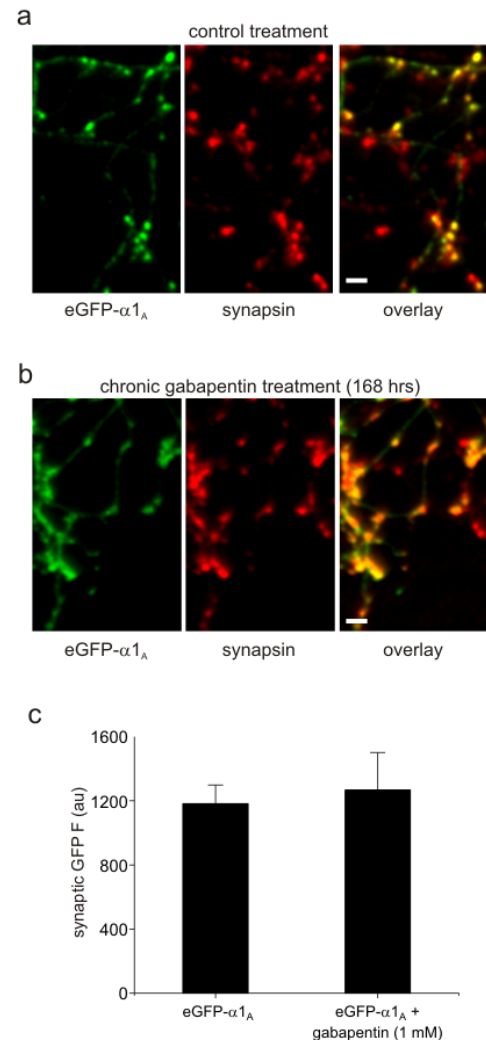


Figure S9. Gabapentin does not impair VGCC trafficking to boutons.

a-b, Confocal immunofluorescence images of neurons transfected with eGFP- $\alpha 1_A$ (on DIV 7 with (a) and without (b) 1mM gabapentin present in incubation medium). Control cells are 14 DIV prior to fixation and stained for GFP (left/green; to identify newly translated $\alpha 1_A$) and synapsin (middle/red; to identify presynaptic terminals). Overlay of two images (right panel). Scale bar = 2 μm . **c** quantification of GFP signal (F) from synaptic boutons for cells incubated with (1182 \pm 116) and without (1267 \pm 233) gabapentin to measure *de novo* trafficking of channels to synaptic boutons; n=6 values are mean \pm SEM.



REFERENCES

1. Winterfield, J. R. & Swartz, K. J. A hot spot for the interaction of gating modifier toxins with voltage-dependent ion channels. *J Gen Physiol* **116**, 637-44 (2000).
2. Ariel, P. & Ryan, T. A. Optical mapping of release properties in synapses. *Front Neural Circuits* **4** (2010).
3. Tian, L. et al. Imaging neural activity in worms, flies and mice with improved GCaMP calcium indicators. *Nat Methods* **6**, 875-81 (2009).